PCCP

Diphenol radical cations and semiquinone radicals as direct products of the free electron transfer from catechol, resorcinol and hydroquinone to parent solvent radical cations

Ortwin Brede,*[a] Sudhir Kapoor,[c] Tulsi Mukherjee,[c] Ralf Hermann[a] and Sergej Naumov[b]

[a] *Interdisciplinary Group for Time-Resolved Spectroscopy, University of Leipzig, Permoserstr. 15, D-4303, Leipzig, Germany. E-mail: brede@mpgag.uni-leipzig.de*
[b] *Institute of Surface Modification, D-4303, Leipzig, Germany*
[c] *Radiation Chemistry and Chemical Dynamics Division, Bhabha Atomic Research Centre, Trombay, Mumbai 400085, India*

Received 14th June 2002, Accepted 20th August 2002
First published as an Advance Article on the web 11th September 2002

In the pulse radiolysis of solutions of catechol, resorcinol and hydroquinone in n-butylchloride, dihydroxybenzene radical cations (40%) as well as semiquinone radicals (60%) are observed as direct synchronously formed products of the electron transfer from the solvent parent ions to the solute. This is explained in terms of free electron transfer succeeding in nearly every encounter of the reactants, which in the case of the studied dihydroxybenzenes involves femtosecond molecular dynamics effects. The rotation of the C–OH bond causes cycling of the molecule through transient conformations also exhibiting different electron distributions. From the more chemical point of view, the diphenol radical cations represent the first and till now unknown intermediates of oxidative semiquinone radical formation.

Introduction

Parent radical cations derived from non-polar solvents (RX) such as n-alkanes, cycloalkenes and alkyl chlorides are very efficient electron acceptors. So they are nearly universal tools for the generation of solute radical cations (S).[1,2]

$$\text{c-}C_6H_{12}{}^{\bullet+},\ \text{n-}C_4H_9Cl^{\bullet+}\ etc. + S \rightarrow S^{\bullet+} + \text{c-}C_6H_{12},\ \text{n-}C_4H_9Cl \ldots \quad (1)$$

This reaction type, free electron transfer (FET),[3] is well studied by pulse radiolysis. Generally, it has been found that the rate of eqn. (1) is governed by diffusion kinetics. But recently it has seemed probable that the real electron jumping step, on a microscopic scale, proceeds over times typical of molecular vibrations, *i.e.* in the range of tenths of femtoseconds.[4] This statement was derived from electron transfer experiments analogous to eqn. (1) using phenols,[5,6] thiophenols[7] and selenols[8] as electron donors. In these cases, using nanosecond pulse radiolysis, we found solute radical cations as well as hetero-centered radicals, for phenols (ArOH) in comparable amounts, see reaction (2).

$$RX^{\bullet+} + Ar\text{–}\theta\text{–}OH \rightarrow \begin{cases} ArOH]^{\bullet+} \\ \rightarrow Ar\text{–}O^{\bullet+}\text{–}H \rightarrow ArO^{\bullet} + H^{+} \end{cases} + RX \quad (2)$$

In reaction (2), it is implied that FET happens during the rotation of the OH group (symbolized by "θ") which has a frequency of around 10^{13} Hz. In the course of this rotation the molecular situation could be understood in terms of two boundary cases, a plane structure and a twisted one (OH group twisted 90 degree out of plane) which should exhibit also different electron distributions.[4] Assuming direct and non-hindered FET, two types of intermediate cations should be formed, *i.e.* a conjugated cation (route (2a)) and an oxygen localized one (route (2b)), where the latter deprotonates immediately.

Now the question arose whether or not the mentioned effect applies also for more functional phenols and, in particular for dihydroxybenzenes such as catechol, resorcinol and hydroquinone. The oxidation of these compounds has been well investigated for a long time and the first step is found to result in semiquinone radicals or their corresponding anionic forms.[9–13] So aside from details of the electron transfer mechanism the existence and properties of possible diphenol radical cations as the real primary oxidation products are of great interest.

Experimental

Pulse radiolysis

The liquid samples were irradiated with a high energy electron pulse (1 MeV, 15 ns duration) generated by a pulse transformer type accelerator ELIT (Institute of Nuclear Physics, Novosibirsk, Russia). The dose delivered per pulse was measured with an electron dosimeter and was usually around 100 Gy unless otherwise stated. Detection of the transient species was carried out using an optical absorption set-up consisting of a pulsed xenon lamp (XBO 900, Osram), a Spectra Pro-500 monochromator (Action Research Corporation), an IP28 photomultiplier (Hamamatsu Photonics) and a 1 GHz digitizing oscilloscope (TDS 640, Tektronix). Further details are given elsewhere.[14]

Unless otherwise stated the pulse radiolysis experiments were carried out in nitrogen-bubbled solutions of n-butyl chloride. The solutions were continuously passed through the sample cell with a path length of 1 cm.

 DOI: 10.1039/b205771a

Data analysis

The lifetimes of the biphenol radical cations were obtained from simple first order exponential regression of the experimental time profiles.

The corresponding rate constants for various paths involved in the decay of the radical cations were used to simulate the decay profiles of biphenols radical cations and its corresponding phenoxyl radicals. Details of the procedure are reported earlier.[4,15]

Chemicals

All the biphenols studied were commercially available (Aldrich). Chlorobutane and 1,2-dichloroethane were obtained from Merck. Triethylamine (Aldrich), dimethylsulfoxide (Aldrich) and triphenylamine (Aldrich) were used as received.

Results

Pulse radiolysis of catechol in non-polar solution

The interaction of ionizing radiation with non-polar solvents results in the generation of sigma-type radical cations which are metastable in the nanosecond timescale.[2] So for n-butyl chloride[16] (n-BuCl) and 1,2-dichloroethane[4] (DCE) cationic transients are observed with broad absorption maxima in the visible peaking around 550 nm and exhibiting maximum lifetimes up to 150 ns.

$$\text{n-}C_4H_9Cl \rightsquigarrow \text{n-}C_4H_9Cl^{\bullet+}, Cl^-, \text{n-}C_4H_9^{\bullet}, \textit{etc.} \qquad (3)$$

As crude information about the driving force of the electron transfer eqn. (1), its free energy can be estimated from the ionization potential difference between the solute and solvent. The gas phase ionization potentials of catechol, resorcinol and hydroquinone are around 8.2 eV,[17] while for the solvents 1,2-dichloroethane and for n-butyl chloride the values are 11.0 eV and 10.7 eV, respectively. Hence, with an enthalpy difference of around 2.5 eV for the gross electron transfer reaction (1) involving the dihydroxybenzenes, diffusion-controlled rate constants are expected and indeed measured.

On pulse-irradiating samples containing catechol, the absorption band of the solvent radical cations disappears with concomitant formation of solute transients with absorption in the wavelength region between 350 and 450 nm, *cf.* Fig. 1. In 10^{-2} mol solution of catechol, according to the transfer rate $k_2 = 10^{10}$ dm^3 mol^{-1} s^{-1} all the product absorption is formed practically within the electron pulse, but caused, however, by different species which can be seen from the lifetimes in different spectral positions, *cf.* the spectra and time profiles given in Fig. 1. So a short living species with $\lambda_{max} = 400$ nm (assigned as radical cation) and a long-lasting one with two bands at $\lambda_{max} = 365$ and 375 nm (assigned to be the catechol semiquinone radical) are distinguishable.

The kinetic identification of the short-living transient was made by adding typical cation scavengers[18] such as dimethylsulfoxide (DMSO) or triethylamine (TEA).

In the presence of DMSO, the time profiles at $\lambda = 390$ nm show an increase in rate, according to a pseudo first order reaction with $k_4 = 1.5 \times 10^{10}$ dm^3 mol^{-1} s^{-1}, see inset in Fig. 2. The difference of the spectra of the 10^{-2} molar catechol solution in the absence and in the presence of 10^{-3} mol dm^{-3} DMSO yielded the absorption band of the catechol radical cation, see Fig. 2. Because DMSO does not cause a marked reduction of the radical absorption we concluded that DMSO causes deprotonation of the radical cation, eqn. (4), rather than electron transfer quenching.

$$HO\text{–}Ar\text{–}OH]^{\bullet+} + DMSO \rightarrow HO\text{–}Ar\text{–}O^{\bullet} + H^+(DMSO) \qquad (4)$$

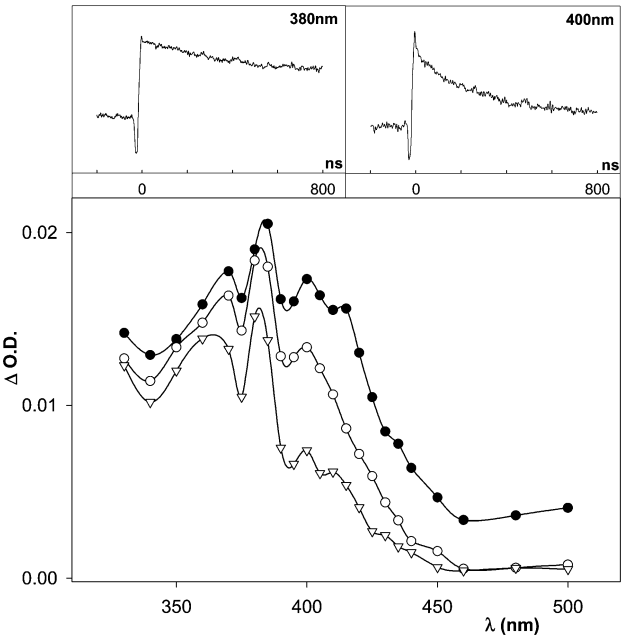

Fig. 1 Transient spectra of the pulse radiolysis of a N_2 purged solution of 10^{-2} mol dm^{-3} catechol in n-butylchloride taken (●) immediately after the pulse and after (○) 30 and (▽) 250 ns. The time profiles demonstrate the kinetic behavior in the absorption maxima.

In contrast, because of its lower ionization potential, TEA acts as an efficient hole and radical cation scavenger:

$$HO\text{–}Ar\text{–}OH]^{\bullet+} + TEA \rightarrow HO\text{–}Ar\text{–}OH + TEA^{\bullet+} \qquad (5)$$

In the presence of millimolar concentrations of TEA, the time profiles at 390 nm show also an increase in rate, but also depletion of the catechol radical absorption (not shown). Concomitantly, around 330 nm the formation of TEA species could be observed. The quenching rate constant was determined as

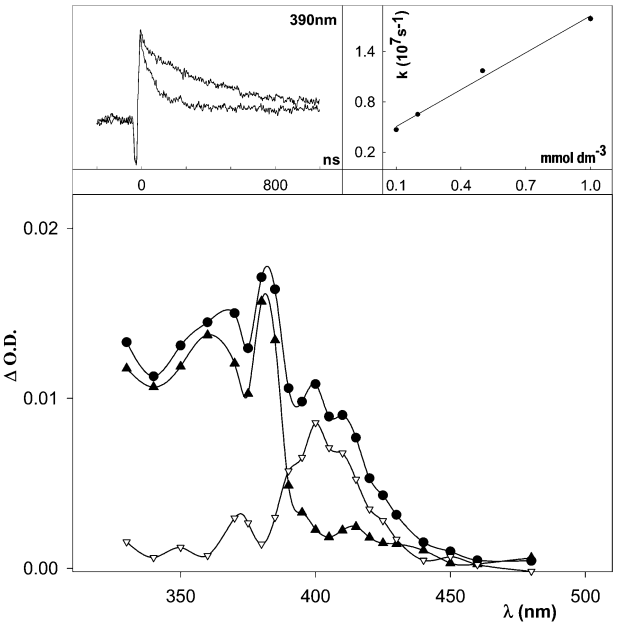

Fig. 2 Transient spectra of a N_2-purged solution of 10^{-2} mol dm^{-3} catechol in n-butylchloride taken 100 ns after the electron pulse: (●) this solution, (△) sample additionally containing 10^{-3} mol dm^{-3} DMSO, (▽) difference spectrum between (●) and (△). The time profile demonstrates the influence of DMSO on the cationic time profile. The Stern–Volmer plot concerns the DMSO quenching reaction, eqn. (4).

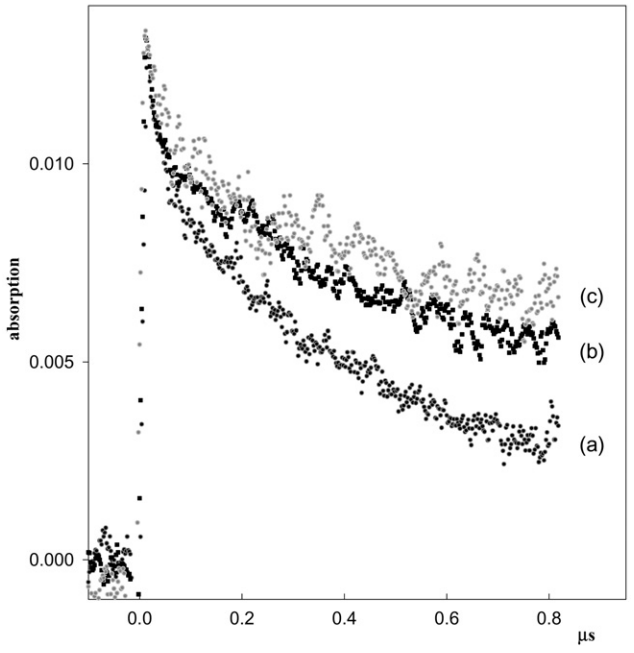

Fig. 3 Effect of different doses per pulse (a: 100 Gy, b: 50 Gy, c: 20 Gy) on the time profile of the catechol radical cation at $\lambda = 400$ nm measured in a solution of 10^{-2} mol dm^{-3} catechol in n-butylchloride.

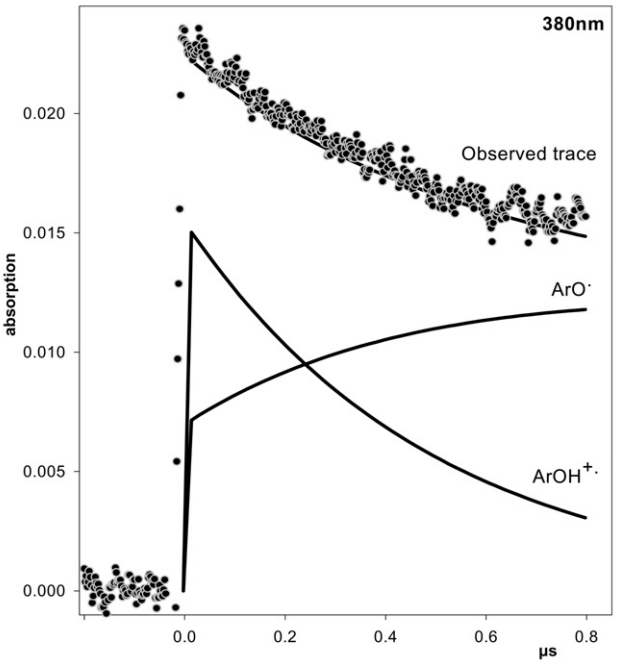

Fig. 4 Example of simulation of the time profiles of superimposed radical cation and phenoxyl radical absorptions with eqns. (8) and (9).

$k_5 = 2\times10^{10}$ dm^3 mol^{-1} s^{-1}. These experiments confirm the transient assignment as stated above.

Analyzing the fate of the observed catechol species, the decay of the radical cation was found to be first order with a lifetime of about 700 ns while the phenoxyl radical decays by second order kinetics. In fact there are various routes by which phenol radical cations can decay, among them quenching reactions, eqns. (4) and (5), deprotonation, eqn. (6), and neutralization, eqn. (7). Although reactions (6) and (7) have probably the same chemical consequence, the charge neutralization process, eqn. (7), can be affected by varying the dose rate, and hence the transient concentration. This is demonstrated in Fig. 3 where the decay profiles of the radical cations exhibit a marked dose rate dependence.

$$\text{HO–Ar–OH}^{\bullet+} + \text{solvent} \rightarrow \text{HO–Ar–O}^{\bullet} + \text{H}^+(\text{solvent}) \quad (6)$$

$$\text{HO–Ar–OH}^{\bullet+} + \text{Cl}^- \rightarrow \text{HO–Ar–O}^{\bullet} + \text{HCl} \quad (7)$$

Though catechol radical cations and their semiquinone radicals are rapidly formed by electron transfer analogous to eqn. (2), there is also delayed generation of the semiquinone radicals according to eqns. (6) and (7), *i.e.* a delayed and time-resolved transformation of the radical cations. Therefore, the measured time profiles represent superimpositions of transients generated by electron transfer, eqn. (2), with subsequent conversion of the radical cations into radicals according to eqns. (6) and (7). This makes direct judging of the ratio of the transients very difficult, in particular because of the unknown extinction coefficients of the transients. But on the bases of the mentioned kinetic connection, fitting the time profiles taken at different wavelengths enables to find the ratio between the primary formed electron transfer products, *i.e.* a semiquantitative analysis of the reaction channels, eqns. (2a) and (2b). This works with an internal calibration taking into account that the primarily formed phenol radicals are directly converted into phenoxyl radicals according to reaction (6). The procedure is described in detail in ref. 4 and based formally on the following differential equations:

$$\text{d}[\text{ArOH}^{\bullet+}]/\text{d}t = k_{2a}[\text{ArOH}][\text{RX}^{\bullet+}] - k_6[\text{ArOH}^{\bullet+}] \quad (8)$$

$$\text{d}[\text{ArO}^{\bullet}]/\text{d}t = k_{2a}[\text{ArOH}][\text{RX}^{\bullet+}] + k_6[\text{ArOH}^{\bullet+}] - k_{10}[\text{ArO}^{\bullet}]^2 \quad (9)$$

$$2\text{ArO}^{\bullet} \rightarrow \text{products} \quad (10)$$

Fig. 4 shows a typical example of the fitting with reasonable parameters taken from the electron transfer gross reaction and those determined at favorable spectral points where one transient dominates. By adjusting the molar absorptivity with the WINSPEC program, the relative yields for catechol radical cation and its phenoxyl radical formed just after the pulse were calculated to be about 40% and 60%, respectively.

For getting a more quantitative idea about the formation of catechol radical cations subsequent electron transfer from triphenylamine (TPA) to the primary formed catechol radical cations was carried out, where TPA has a marked lower ionization potential[19] and a known extinction coefficient[20] of TPA$^{\bullet+}$ of $\varepsilon = 2.9\times10^4$ dm^3 mol^{-1} cm^{-1}. Fig. 5 shows the formation of the TPA radical cation after electron pulse irradiating a solution containing 0.01 mol dm^{-3} catechol and 5×10^{-4} mol dm^{-3} TPA in n-BuCl where we can assume complete transformation, eqn. (11). Then the yield of TPA radical cation obtained in a solution without catechol under conditions of complete electron transfer, eqn. (12), was measured (Fig. 5, upper spectrum). Since the experiments were done under identical conditions one can estimate the yield of catechol radical cation formed by electron transfer to the solvent, eqn. (2a) as well as the extinction coefficients of the different catechol species, *cf.* Table 1.

$$\text{HO–Ar–OH}]^{\bullet+} + \text{TPA} \rightarrow \text{TPA}^{\bullet+} + \text{HO–Ar–OH} \quad (11)$$

$$\text{RX}^{\bullet+} + \text{TPA} \rightarrow \text{TPA}^{\bullet+} + \text{RX} \quad (12)$$

The estimated yield of the radical cation was found to be 42% which agrees well with the value derived from the fit procedure mentioned above. Thus, one can conclude that the remaining amount of the solvent parent radical cations *via* eqn. (2b) leads to the formation of catechol phenoxyl radicals, *i.e.* about 58%.

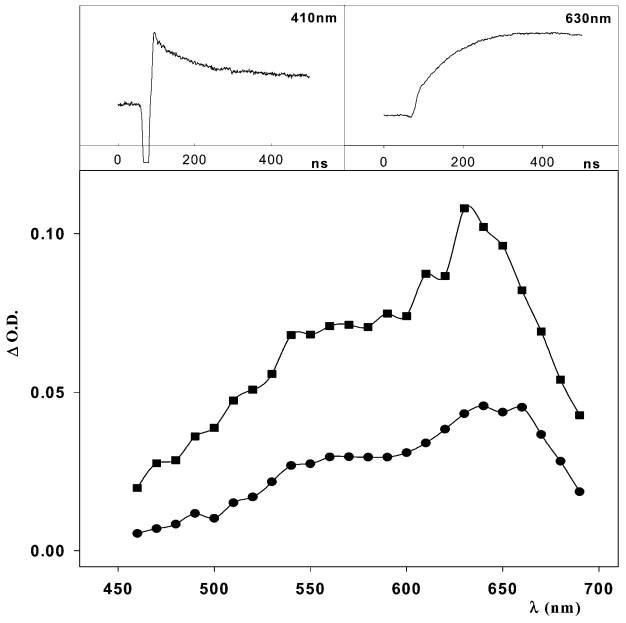

Fig. 5 Calibration of the diphenol radical cation yield: Transient absorption spectra taken 400 ns after pulsing samples consisting in (■) 10^{-2} mol dm^{-3} TPA in n-BuCl (direct reaction (12)), and (●) 10^{-2} mol dm^{-3} catechol and 5×10^{-4} mol dm^{-3} TPA solved in n-BuCl (stepwise electron transfer, reactions (2a) and (11)). The time profiles show typical kinetics of the stepwise transfer measured with the latter sample.

Concerning the fate of the catechol semiquinone radicals, the bimolecular and second order deactivation was found to be much faster as known for aqueous systems. That can be explained by a modified mechanism where instead of disproportionation (eqn. (13), as in aqueous solution[11]) a recombination with the radiolytically formed excess of butyl radicals happens, as described by reaction (14). This is derived from the different product characteristics: in our experiments no *o*-benzoquinone ($\lambda_{max} = 390$ nm) was found, however, the visible bands of the semiquinone at 360 and 380 nm could be seen (*cf.* Fig. 1), which in aqueous solution are covered by the *o*-benzoquinone band.[11] The time profiles given in Fig. 6 show the radical transformation in the 200 μs time range: at 410 nm spike absorption partially of the catechol radical cations, at 370 nm decay of the semiquinone radicals under product formation (background) and at 330 superimposed signal of radical decay and product absorptions, both in equal part. This seems to be consistent with a reaction sequence of eqns. (7) and (14).

$$2\ \text{HO–Ar–O}^{\bullet} \rightarrow \text{HO–Ar–OH} + \textit{o}\text{-quinone}, \quad k_{13} = 1.1 \times 10^{7}\ \text{dm}^3\ \text{mol}^{-1}\ \text{s}^{-1} \qquad (13)$$

$$\text{HO–Ar–O}^{\bullet} + \text{n-C}_4\text{H}_9^{\bullet} \rightarrow \text{HO–Ar–O–C}_4\text{H}_9, \quad k_{14} = 2 \times 10^{9}\ \text{dm}^3\ \text{mol}^{-1}\ \text{s}^{-1} \qquad (14)$$

But in the presence of oxygen the butyl radicals are eliminated by formation of less reactive peroxyl radicals (reaction 15) and, therefore, the lifetime of the semiquinone radicals is considerably prolonged. Applying the disproportionation rate given by Land,[11] under our conditions, however, the semiquinone radical is oxidized by the butylperoxyl radicals according to reaction eqn. (16). This is demonstrated by the time profile given in Fig. 6d. The shown growth was found to be independent on the dose per pulse which excludes reaction (13) and could reasonably explain eqn. (16), taking into account a high excess of the peroxyl radicals.

$$\text{n-C}_4\text{H}_9^{\bullet} + \text{O}_2 \rightarrow \text{n-C}_4\text{H}_9\text{OO}^{\bullet},\ k_{15} = 2 \times 10^{9}\ \text{dm}^3\ \text{mol}^{-1}\ \text{s}^{-1} \qquad (15)$$

$$\text{n-C}_4\text{H}_9\text{OO}^{\bullet} + \text{HO–Ar–O}^{\bullet} \rightarrow \textit{o}\text{-quinone} + \text{n-C}_4\text{H}_9\text{OO}^{-}, \quad k_{16} \approx 10^{8}\ \text{dm}^3\ \text{mol}^{-1}\ \text{s}^{-1} \qquad (16)$$

By the way and as expected, electron transfer, eqn. (2), has not been found to be influenced by oxygen.

FET with resorcinol and hydroquinone

Fig. 7 shows transient absorption spectra and selected time profiles obtained in the pulse radiolysis of N_2-bubbled n-BuCl solution containing 2×10^{-3} mol dm^{-3} *resorcinol*. According to the relatively low resorcinol concentration, the spectrum taken immediately after the pulse is dominated by residual n-BuCl$^{\bullet+}$ absorption, *cf.* also time profile taken at 520 nm. After its decay finished in 50 ns, however, the spectrum exhibits marked absorption bands of resorcinol transients at $\lambda = 405$, 420 and 465 nm which were formed concomitantly as already described for catechol. Whereas the peak at 465 nm decreases with time as typical for a radical cation, no significant decrease of the bands absorbing at 405 and 425 nm could be observed at identical time scale.

Although resorcinol is a *meta*-dihydroxybenzene where no oxidation into a quinone is imaginable, the transient reaction behavior was observed to be quite similar to that of catechol.

In the presence of TEA, the decay rate of the cation absorption band at 465 nm was found to increase according to an electron transfer analogous to eqn. (5), exhibiting a rate constant of $k_5 = 1.4 \times 10^{10}$ dm^3 mol^{-1} s^{-1}. From this experiment we could easily get the absorption spectrum of the resorcinol radical cation by subtracting the absorption spectrum taken in the presence and absence of TEA. It can be seen from Fig. 8 that the resorcinol radical cation has an absorption maximum at 460 nm while the corresponding phenoxyl radical shows peaks at 400 and 425 nm which is similar to that

Table 1 Experimental data obtained for the FET from dihydroxybenzenes to solvent parent radical cations: QH_2 means dihydroxybenzene, ε calibrated on that of TPA$^{\bullet+}$, ref. 20

	Catechol	Resorcinol	Hydroquinone
$QH_2^{\bullet+}$	$\varepsilon_{425} = 1.2 \times 10^4$ dm^3 mol^{-1} cm^{-1}	$\varepsilon_{465} = 1.7 \times 10^4$ dm^3 mol^{-1}cm^{-1}	$\lambda_{max} = 425$ nm
$QH^{\bullet}$	$\varepsilon_{365} = 6300$, $\varepsilon_{375} = 6700$ dm^3 mol^{-1} cm^{-1}	$\varepsilon_{425} = 8600$ dm^3 mol^{-1} cm^{-1}	$\lambda_{max} = 400$ nm
k_2 of FET/dm^3 mol^{-1} s^{-1}	10^{10}, in n-BuCl	10^{10}, in n-BuCl	5×10^9, in DCE
Quenching rates: k_4 (DMSO), k_5 (TEA)/dm^3 mol^{-1} s^{-1}	1.5×10^{10} 2.0×10^{10}	1.0×10^{10} 1.4×10^{10}	Not determined because of strong spectral super-imposition
Ionization potentials from the literature,[17] our calculations (HOMO, vacuum)	8.18 eV, 8.10 eV	8.30 eV, 8.26 eV	7.94 eV, 7.95 eV
τ of $QH_2^{\bullet+}$/ns	700	700	500
$QH_2^{\bullet+}/QH^{\bullet}$ ratio *via* fit (8,9), via TPA expression,eqn. (11)	40/60, 42/58	40/60	40/60

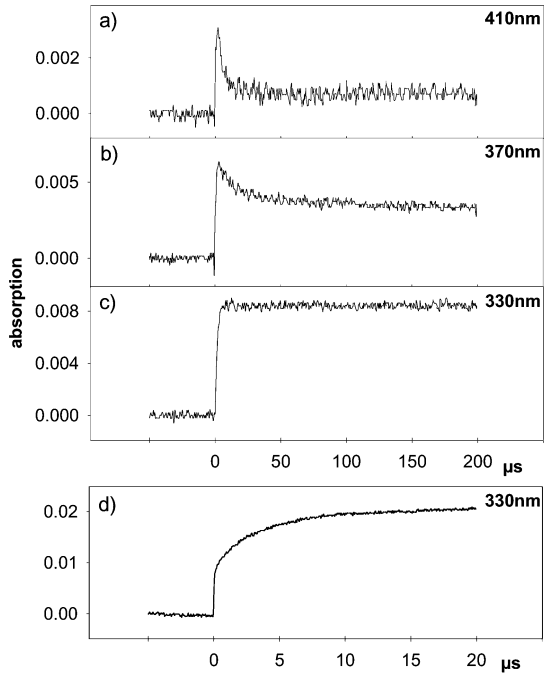

Fig. 6 Time profiles indicating the fate of the catechol transients in a solution of 5×10^{-3} mol dm^{-3} catechol in n-BuCl, N_2 purged: (a) dominating radical cation, (b) decay of the semiquinone, (c) stable product, where (b) and (c) are superimpositions of transient absorptions. (d) Time profile indicating the conversion of the semiquinone radical in the presence of oxygen, according to reaction (16). The sample consisted of a solution of 2×10^{-3} mol dm^{-3} catechol in n-BuCl, purged with oxygen.

reported in water.[13,15] The lifetime of the radical cation was found to be about 700 ns, *i.e.* the species is more stable than those derived from phenols.

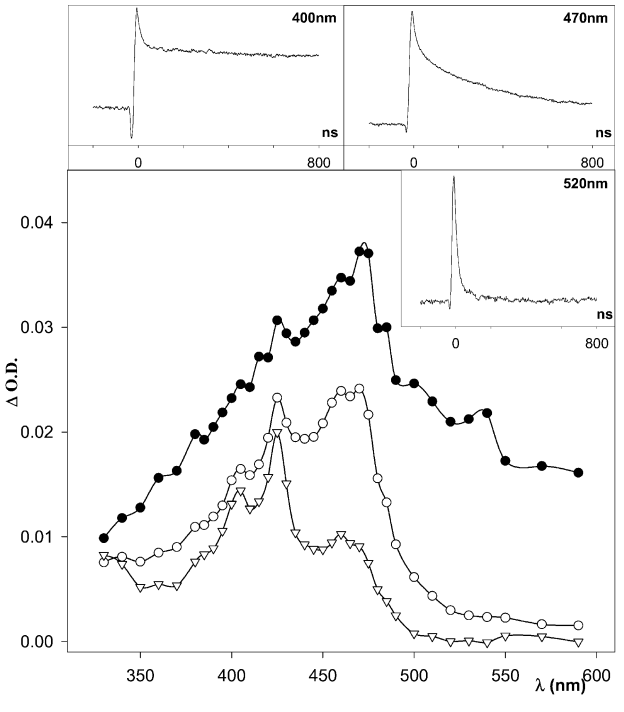

Fig. 7 Transient spectra of the pulse radiolysis of a N_2-purged solution of 2×10^{-3} mol dm^{-3} resorcinol in n-butylchloride taken (●) immediately after the pulse and after (○) 50 and (▽)550 ns. The time profiles demonstrate the kinetic behavior near to the absorption maxima. Spectrum (●) contains a considerable contribution of residual solvent radical cation.

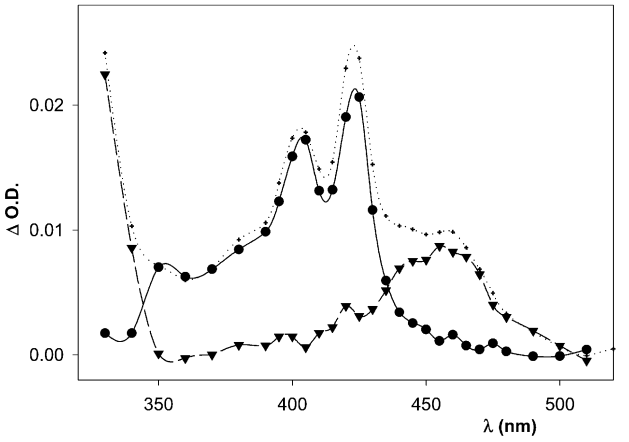

Fig. 8 Transient spectra taken 550 ns after electron pulsing of a solution of 5×10^{-3} mol dm^{-3} resorcinol in n-BuCl, purged with nitrogen in the absence (●) and in the presence of 5×10^{-4} mol dm^{-3} TEA. (▼) represents the difference between these spectra indicating the shape of the resorcinol radical cation spectrum.

Adding millimolar concentrations of DMSO, a rapid conversion of the resorcinol cations into the corresponding phenoxyl according to the deprotonation (4) happens. Fig. 9 shows this effect on hand of time profiles taken at $\lambda = 425$ nm, *i.e.* within the maximum of the phenoxyl radical. In the presence of DMSO a time-resolved growth to a higher amplitude can be seen which enables us to estimate a rate constant k_4 around 10^{10} dm^3 mol^{-1} s^{-1}.

The neutralization of the resorcinol radical cations, eqn. (7), as well as the electron transfer involving TPA, eqn. (11), proceed in the same manner as described for catechol and, therefore, are not documented here (*cf.* Table 1). Also the deactivation of the phenoxyl radicals according to reaction (14) proceeds with a diffusion-controlled rate k_{14} of about 3×10^9 dm^3 mol^{-1} s^{-1}.

Because of the low solubility of *hydroquinone* in n-BuCl of $\leqslant 10^{-3}$ mol dm^{-3}, the electron transfer experiments with it were carried out in 1,2-dichoroethane where in principle the same processes should proceed. Fig. 10 shows transient absorption spectra obtained in the pulse radiolysis of a deaerated solution of 10^{-2} mol dm^{-3} hydroquinone in 1,2-dicholoroethane. Although much more superimposed as in the cases of the other biphenols, we can distinguish a hydroquinone radical cation ($\lambda = 425$ nm) and a phenoxyl radical ($\lambda = 400$ nm) absorption band. The kinetics of these species

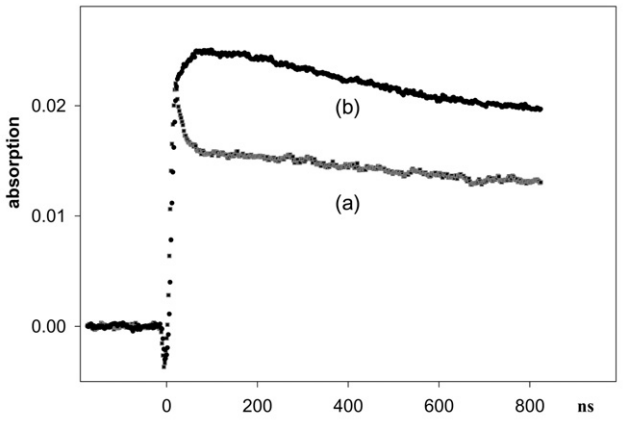

Fig. 9 Time profiles taken at 425 nm of (a) N_2 purged solution of 2×10^{-3} mol dm^{-3} resorcinol in n-BuCl and (b) after adding 10^{-2} mol dm^{-3} DMSO.

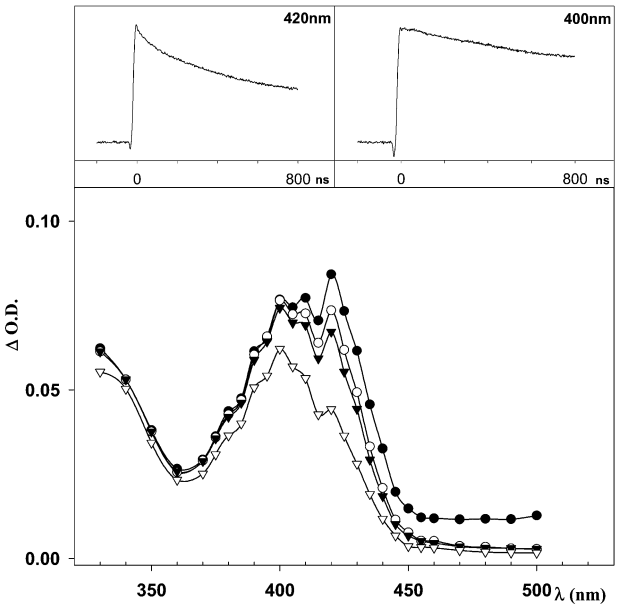

Fig. 10 Transient spectra of the pulse radiolysis of a N_2-purged solution of 10^{-2} mol dm^{-3} hydroquinone in 1,2-dichloroethane taken (●) immediately after the pulse and after (○) 50, (▼) 100 and (▽) 550 ns. The time profiles demonstrate the kinetic behavior near to the absorption maxima.

follow the same rules as described for the other dihydroxybenzene isomers, *i.e.* that

(*i*) the hydroquinone radical and radical cation were formed synchronously by electron transfer, eqn. (2a) and (2b) in a ratio of 60 : 40 calculated from the TPA reaction, eqn. (11), and

(*ii*) the quenching experiments with DMSO, eqn. (4), and TEA, eqn. (5), gave analogous results (*cf.* Table 1).

Although for the oxidation of hydroquinone in aqueous solution not in each case it could be well distinguished between semiquinone radical and its anionic form,[10,11,13,22] here we can state that the 400 nm species is really the radical form.

Discussion

As already reported for the ionization of various monofunctional phenols[4] by free electron transfer to solvent parent ions, also for all of the bifunctional hydroxybenzenes such as catechol, resorcinol and hydroquinone the product splitting into radical cations and phenoxyl radical was observed. In variation of the introducingly formulated FET reaction, eqn. (2a) and (2b), this is formulated for the biphenols in reaction (17a) and (17b):

$$RX^{\bullet+} + HO\text{–}\theta\text{–}Ar\text{–}\theta\text{–}OH \rightarrow \begin{cases} \text{planar state} \rightarrow HOArOH]^{\bullet+} \\ \text{twisted state} \rightarrow (HOAr\text{–}O^{\bullet+}\text{–}H) \rightarrow HOArO^{\bullet} + H^{+} \end{cases} + RX \quad (17)$$

(θ) symbolizes here the rotation of at least one C–θ–OH group around the indicated axis. So in the approach of the reactants by diffusion, an adiabatic and immediate electron jump happens over times comparable to or shorter than the rotational frequency. As indicated in eqn. (17) and by analogy with the monofunctional phenols, because of the rotation of the C–OH bond at least two boundary cases could be defined: one with the molecule in plane and the other one with a twisted bond (90 degree out of plane). Now it was interesting to reason this behavior by looking on the dynamics of the diphenol molecule combined with the changes of the electron distribution in the three highest MO's, to consider the stability of the formed radical cations and to compare it with the monofunctional phenols. Hence we performed quantum-chemical calculations on these problems.

Calculations on the molecular dynamics of biphenols

Quantum chemical calculations were done using the Gaussian 98, Revision 11 program package.[23] The equilibrium geometries of the structures investigated were optimized without any restriction. The atomic charges as well as the atomic spin densities were calculated using the Mulliken population analysis. The Hartree–Fock (HF) and hybrid density functional theory (DFT) B3LYP[24–26] methods were used for the investigation of the geometrical parameters and electronic structures of the dihydroxybenzene ground state singlet and cation radical. All methods show the similar influence of the molecular geometry on electronic structure. The frequency calculations were used to locate transition state geometries, to determine the nature of stationary points found by geometry optimization, and to obtain thermochemistry parameters such as zero-point energy (ZPE), thermal correction to energy (TE) and activation energy E_a (height of rotation barrier). The calculated data for the frequency analysis and thermochemical parameters are given in Tables 2. The B3LYP/6-31G(d) method was used because DFT is superior to other methods in reproducing the vibrational frequencies for phenols.[27] E_a were calculated as difference between $E_0 + ZPE + TE$ of the stable and transition state (TS) structures of the molecules.

As for phenol the frequency calculations on the hydroquinone and resorcinol stable planar structures produce no negative frequencies indicating that this conformation is at an energy minimum, whereas structures with one O–H group perpendicular to the ring plane (about 90°) produce only one negative (imaginary) frequency indicating that these conformations are first–order saddle points (transition states).

The calculations on the catechol resulted in some different properties. In the stable planar structure there is a strong

Table 2 B3LYP/6-31G(d) calculated thermochemistry parameters for stable and transition states. ν_{min} is the minimal calculated frequency. ν_{rot} and ν_{val} are rotation and valence vibrational frequencies of OH-group. E_a is the activation energy of the OH group rotation. For comparison data for ordinary phenol are also given.

	ν_{min}/cm^{-1}	Structure	ν_{rot}/cm^{-1}	ν_{val}/cm^{-1}	$E_0 + ZPE + TE$/a.u.	E_a/kcal mol^{-1}
Phenol plane	+234	Minimum	359	3751	−307.3546	3.2
Ar–OH 90°	−351	Transition state			−307.3494	
1,4-dOH–Ar plane	+158	Minimum	314	3758	−382.5628	2.3
Hydroquinone 90°	−299	Transition state			−382.5591	
1,3-dOH–Ar plane	+228	Minimum	350	3753	−382.5651	2.9
Resorcinol 90°	−368	Transition state			−382.5604	
1,2-dOH–Ar plane	+188	Minimum	427	3717	−382.5628	3.3
Catechol 40.9°	−205	Transition state			−382.5608	

interaction between one oxygen atom and the hydrogen atom of the neighbour OH group shortening the distance OH···O to only 0.212 nm. This interaction influences the transition state geometry by OH twisting out of plane of about 41°.

As can be noted from Table 2, the valence O–H oscillations are at least 10 times faster than the rotation of the C–OH group, but both of them are postulated to be slower as the electron transfer jump. It should be mentioned that our data of the phenol molecular oscillations are compatible with those given by Qin and Wheeler.[28]

Because of the small activation energies (barrier heights) E_a for all studied molecules, internal rotation of OH-groups is possible. But within the Born–Oppenheimer approximation the molecular geometry is rigid compared to electron relaxation processes and very fast electron transfer events.

It is known that the molecular orbital (MO) description can be used also for the interpretation of chemical phenomena. Though, checking the effect of the molecular geometry on the electronic structure, we investigated the behaviour of the highest doubly-occupied MO's (HOMO) of the dihydroxybenzene singlet ground state, which certainly are involved in the electron transfer process, with respect to OH-group rotation (measured by the torsion angle), *cf.* Fig. 11.

Following the same principles as phenol,[4] the HOMO is stabilized and drops down with an out-of-plane bond twisting, the HOMO-1 is not influenced by bond twisting, and concomitantly the HOMO-2 level rises due to the strong electron localization on the oxygen atom in the perpendicular structure. Thus, if one of the both OH groups is perpendicular to the aromatic ring, the three highest doubly-occupied molecular orbitals are closer to each other, *i.e.*, the ionization potential differences become smaller.

Electron transfer from donor (biphenol) to acceptor ($BuCl^{+\bullet}$) can be treated in terms of chemical reactivity[29,30] as the direct interaction between overlapping orbitals. Depending on the energy difference ($\Delta\varepsilon$) between the highest occupied MO's of the donor and the lowest empty orbital of the acceptor, the reaction can be either charge controlled or frontier orbital controlled. In case of biphenols $\Delta\varepsilon$ is very small for all three HOMO's and, therefore, interactions between the frontier orbitals are predominant. This is the case of a frontier orbital controlled reaction and strongly coupled electron transfer occurs between them under the assumption of good overlap.

As shown in Fig. 12 for the case of hydroquinone, in the planar structure all three doubly-occupied MO's have the same π-symmetry with strongly delocalized electrons. In contrast, if one of the OH groups is perpendicular to the molecular plane, only HOMO and HOMO-1 are delocalized whereas HOMO-2 exhibits n-symmetry and is strongly localized on the oxygen atom. Similar dependence of the MO's on C–OH group rotation was found for the other biphenols.

Considering the MO scheme of a neutral closed shell biphenol molecule (Fig. 12), the ground configuration (a) and the excited configuration (b) of the corresponding radical cation (Koopman's configurations) can be achieved by a one step electron transfer.[31] By a phenomenological comparison of the planar and the perpendicular structures it can be seen that only the long-lasting, stable and delocalized radical cation can be derived from the planar structure whereas in the perpendicular situation, because of the excess energy and the relatively small ionization potential difference, electron transfer could happen also from HOMO-2, *i.e.* from the localized structure. Moreover, in the actual case because of the strong localization of the HOMO-2 electron, the overlap (and the charge transfer integral) between the MO's of the reactants is about twice as large as the overlap involving the HOMO and results in a favourable interaction energy. Though the hypotheses of the electron transfer from HOMO-2 combined with the formation of a oxygen localized radical cation in the perpendicular structure seems to be justified.

Mechanistic consequences

Relating to these results, within a sufficiently short time scale where the rotation of the critical bond C–OH is "frozen" (femtosecond range) we can assume two borderline conformer structures, strongly differing in the tendency towards prompt dissociation after ionization, corresponding to eqn. (17a) and (17b). Whereas the heteroatom-localized radical cation (with O–H vibration frequency) dissociates immediately to a phenoxyl radical, eqn. (17b), the delocalized planar radical cation eqn. (17a) represents a species which is metastable on

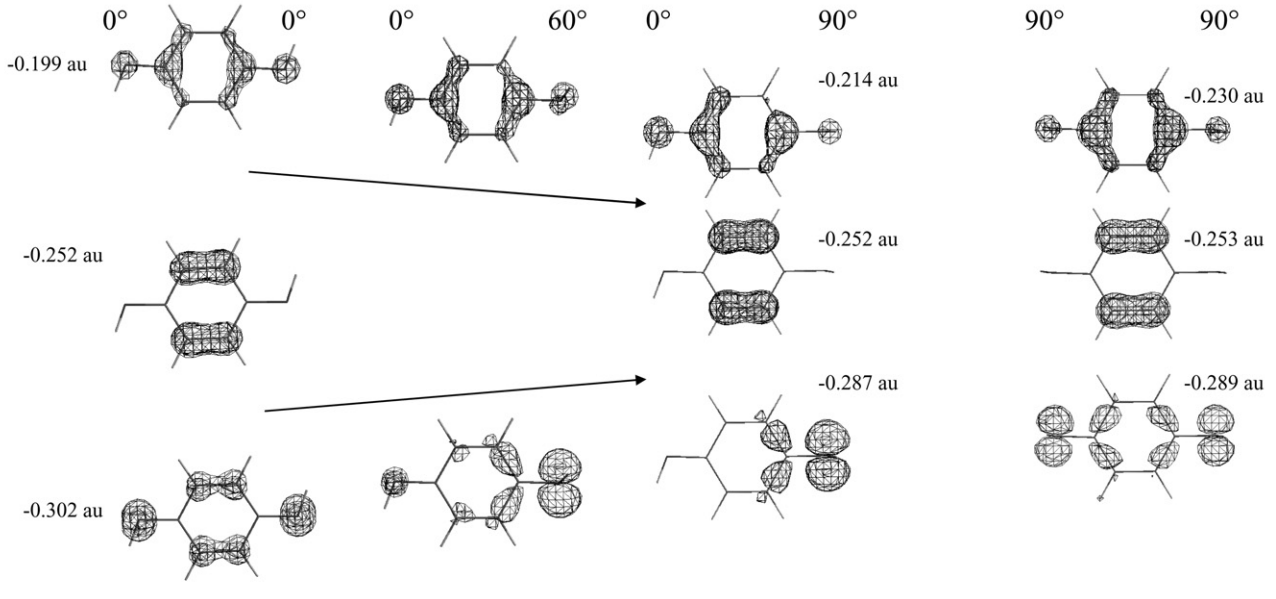

Fig. 11 Transformation of HOMO, HOMO-1 and HOMO-2 of the hydroquinone singlet ground state (isocontour = 0.08) with respect to the deviation of the OH-groups out of the molecular plane as calculated with B3LYP/6-31G(d).

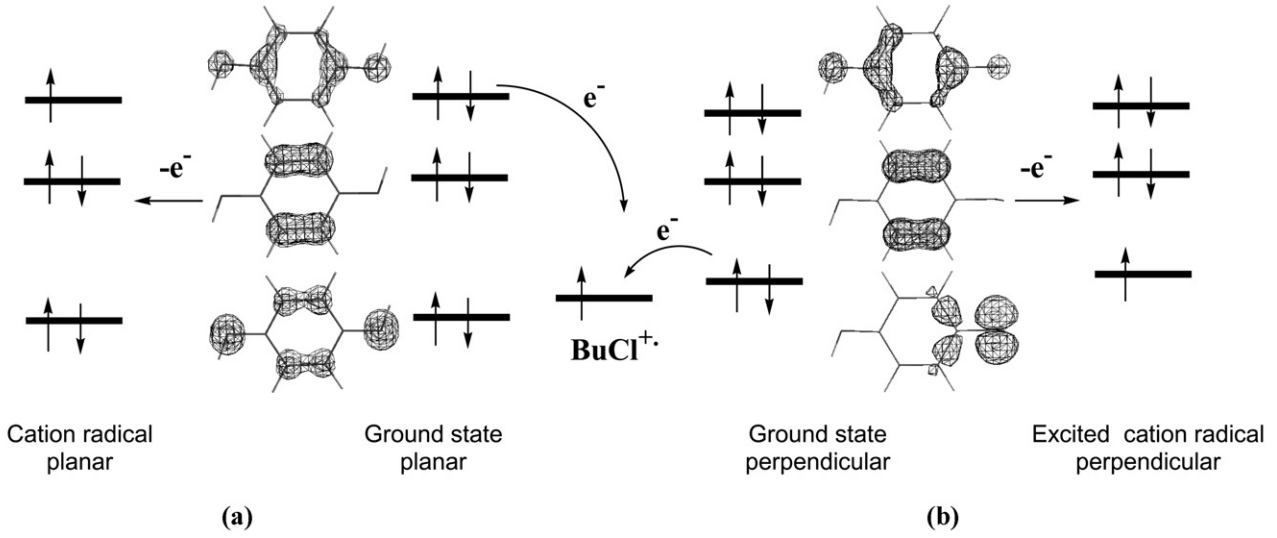

Fig. 12 Molecular orbital scheme of the electronic configurations of the cation radicals formed by electron transfer from the planar (a) and perpendicular (b) hydroquinone singlet ground state molecule to the solvent radical cation.

a timescale of some hundred nanoseconds. Afterwards it deprotonates in a delayed manner, eqn. (6).

Surprisingly, the metastable dihydroxybenzene cation is more stable as found for the radical cations derived from most of the monofunctional phenols. Table 3 and Fig. 13 show correlations of the experimentally determined lifetimes of the phenol radical cations with quantum chemical calculated parameters such as atom spin density on oxygen S(O) and the Mulliken charge difference on the OH group between the singlet ground state and the cation radical. So for S(O) and ΔQ(OH) reasonable plots were found exhibiting correlation coefficients around 0.9. The greater the unpaired electron density on oxygen, the shorter the experimental lifetime of the radical cation was found to be. And certainly, for the phenols the lifetimes depend strongly on the electron-withdrawing or donating properties of further substituents.

Concerning the probability of the appearance of products according to eqn. (17), under the assumption that only the unsymmetrical mono-twisted biphenol rotational situation should lead to the unstable localized cation structure, the yield of the rapidly formed phenoxyl radicals should be higher, as for simple phenols, where a value of 50% has been found. Indeed, in accordance with a simple probability estimation, the experiments described in this paper give a general product distribution ratio of 60% phenoxyl and 40% radical cation.

A salient feature of the present study is the observation of radical cations of the three dihydroxybenzene isomers. Just for the *ortho*- and *para*-derivative these cations represent the hitherto unobserved first products of the well known stepwise one electron oxidation of diphenols to quinones, eqn. (18), where the direct formation of the semiquinone radical has been claimed till now. So these experiments in non-polar solvents show that the self-deprotonation of the metastable delocalized biphenol radical cations is a relatively delayed process. But adding more polar substances, *e.g.*, DMSO, we could demonstrate diffusion-controlled deprotonation, eqn. (4), which certainly happens also in water and other protic solvents as a very rapid and therefore covered process. Recently, this deprotonation behavior has been extensively studied for a variety of monofunctional phenols.[18]

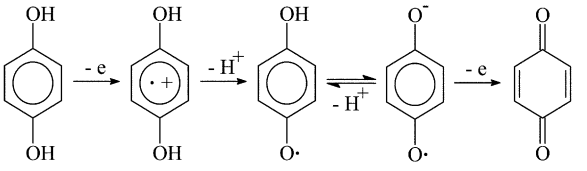

(18)

Table 3 DFT B3LYP/6-31G(d)/SCRF = Dipole(ε = 8) calculated atomic spin density on oxygen S(O) and Mulliken charge differences on OH group between singlet ground state and cation radical ΔQ(OH) different substituted phenols in comparison with the experimentally obtained lifetimes τ/ns, of the phenol radical cations in BuCl.

Phenols	τ/ns	S(O)	ΔQ(OH)
4-CN–ArOH	110	0.204	0.204
4-NO_2–ArOH	230	0.242	0.241
ArOH	270	0.201	0.213
4-Cl–ArOH	320	0.189	0.203
4-MeO–ArOH	340	0.153	0.176
4-HO–ArOH	500	0.162	0.179
4-NH_2–ArOH	680	0.118	0.136
2-HO–ArOH	700	0.149	0.178
3-HO–ArOH	700	0.106	0.155
4-NMe_2–ArOH	1160	0.103	0.133
3-NMe_2–ArOH	1270	0.003	0.084

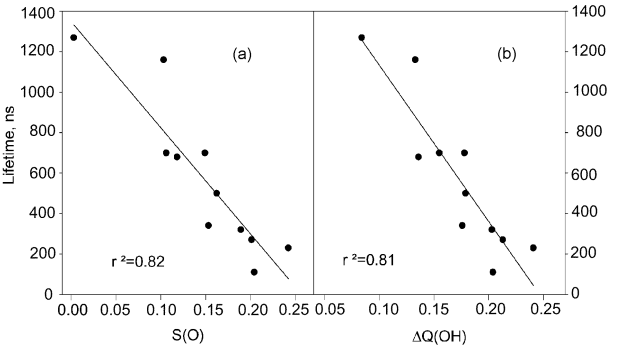

Fig. 13 Correlation of the experimentally obtained lifetimes τ/ns of the different substituted phenol radical cations in BuCl with the quantum chemical parameters: (a) atomic spin density on oxygen S(O) (b) Mulliken charge difference on OH group between singlet ground state and cation radical ΔQ(OH) as calculated at DFT B3LYP/6-31G(d)/SCRF = Dipole(ε = 8)

Conclusion

By analogy with phenols, thiols and selenols, by free electron transfer from the bifunctional phenols catechol, resorcinol and hydroquinone to parent radical cations derived from non-polar solvents (alkanes, alkyl chlorides), diphenol radical cations as well as phenoxyl radicals in the ratio 2:3 are formed as directly observable products. Although the detection time was limited to $\geqslant$10 ns, we are stating that within the electron transfer gross process eqn. (17), the electron jump proceeds in times of $\leqslant$10 fs and, therefore, diffusion only determines the time scale of transient observation in so far that reactants must be brought together for reaction. The very rapid electron jump proceeds in times faster than the molecular oscillations of the electron donor molecule and, hence, identifies the molecular situation of at least C–OH bond rotation.

The formed biphenol radical cations are converted in the 500 ns time range into phenoxyl radicals, eqn. (18), but they were found to be more stable than those of the monofunctional phenols (see Tables 1 and 3). As related to the biologically and electrochemically interesting stepwise oxidation of hydroquinone (catechol) into the corresponding quinones by subsequent one-electron transfers, here we could observe the primary biphenol radical cation directly which has been ignored until now.

References

1 R. Mehnert, in *Radical Ionic Systems – Properties in Condensed Phases*, ed. A. Lund and M. Shiotani, Kluwer, Dordrecht, 1991, p. 231.
2 O. Brede, R. Mehnert and W. Naumann, *Chem. Phys.*, 1987, **115**, 279.
3 O. Brede, *Res. Chem. Intermed.*, 2001, **27**, 549.
4 O. Brede, R. Hermann, W. Naumann and S. Naumov, *J. Phys. Chem.A*, 2002, **106**, 1398.
5 O. Brede, M. R. Ganapathi, S. Naumov, W. Naumann and R. Hermann, *J. Phys. Chem. A*, 2001, **105**, 3757.
6 O. Brede, H. Orthner, V. Zubarev and R. Hermann, *J. Phys. Chem.*, 1996, **100**, 7097.
7 R. Hermann, G. R. Dey, S. Naumov and O. Brede, *Phys. Chem. Chem. Phys.*, 2000, **2**, 1213.
8 O. Brede, R. Hermann, S. Naumov and H. S. Mahal, *Chem. Phys. Lett.*, 2001, **350**, 165.
9 S. Patai, *The Chemistry of Quinoid Compounds*, Wiley, N.Y., 1974, vol. I and II.
10 G. E. Adams and B. D. Michael, *Trans. Faraday Soc.*, 1967, **63**, 1171.
11 E. J. Land, *J. Chem. Soc., Faraday Trans.*, 1993, **89**, 803.
12 R. E. Huie and P. Neta, *J. Phys. Chem.*, 1985, **89**, 3918.
13 V. A. Roginsky, L. M. Pisarenko, W. Bors, C. Michael and M. Saran, *J. Chem. Soc., Faraday Trans.*, 1998, **94**, 1835.
14 O. Brede, F. David and S. Steenken, *J. Chem. Soc., Perkin Trans. 2*, 1995, 23.
15 M. R. Ganapathi, R. Hermann, S. Naumov and O. Brede, *Phys. Chem. Chem. Phys.*, 2000, **2**, 4947.
16 R. Mehnert, O. Brede and W. Naumann, *Ber. Bunsen-Ges. Phys. Chem.*, 1982, **86**, 525.
17 M. Gerhards, C. Unteberg and S. Schumm, *J. Chem. Phys.*, 1999, **111**, 7965.
18 M. R. Ganapathi, S. Naumov, R. Hermann and O. Brede, *Chem. Phys. Lett.*, 2001, **337**, 335.
19 S. L. Murov, I. Carmichael, G.L. Hugh, *Handbook of Photochemistry, 2nd edition,* Marcel Dekker, N.Y. 1993.
20 H. D. Burrows, D. Greatorex and T. J. Kemp, *J. Chem. Phys.*, 1966, **44**, 2369.
21 S. Steenken and P. Neta, *J. Phys. Chem.*, 1982, **86**, 3661.
22 K. B. Patel and R. L. Willson, *J. Chem. Soc., Faraday Trans. 1*, 1973, **69**, 814.
23 M.J. Frisch *et al.*, *Gaussian 98, Revision A9*, Gaussian Inc., Pittsburgh PA, 1998.
24 A. D. Becke, *J. Chem. Phys.*, 1993, **98**, 5648.
25 A. D. Becke, *J. Chem. Phys.*, 1996, **104**, 1040.
26 Ch. Lee, W. Yang and R. G. Parr, *Phys. Rev. B*, 1987, **37**, 785.
27 W. Zierkiewicz, D. Michalska and T. Zeegers-Huykens, *J. Chem. Phys.*, 2000, **104**, 11 685.
28 Y. Quin and R. A. Wheeler, *J. Phys. Chem.*, 1996, **100**, 10 554.
29 G. Klopman, *J. Am. Chem. Soc.*, 1968, **90**, 223.
30 L. Salem, *J. Am. Chem. Soc.*, 1968, **90**, 543.
31 T. Bally, in *Radical Ionic Systems – Properties in Condensed Phases*, ed. A. Lund and M. Shiotani, Kluwer Dordrecht, 1991, p. 4.